เนื้อหางานวิจัย

Introduction

Metal-catalyzed controlled/living radical polymerization (LRP)[1] first reported by Otsu in 1990 has become one of the most widely investigated polymerization techniques. Examples of metal-catalyzed LRP include atom transfer radical polymerization (ATRP)[2,3] and single electron transfer-living radical polymerization (SET-LRP).[4,5] Advantages of these processes include high functional group tolerance and an ability to afford polymers with controlled molecular weights, well-defined architectures, and narrow molecular weight distributions.[6-11] Despite these favorable characteristics, a major limitation associated with normal copper-catalyzed ATRP is the sensitivity to oxygen from air, which can inhibit polymerization as a result of irreversible oxidation of Cu^{I} or formation of inactive peroxy radicals.[12] In addition, for certain systems, an overly active Cu^{I} catalyst rapidly converts to the persistent radical Cu^{II}-X and generates a high concentration of propagating radicals (R•).[9] This event inevitably leads to radical termination and consequently large polymer masses with low monomer conversions.[13]

In comparison, SET-LRP, which features a heterogeneous Cu^{0} in the polymerization system, is more tolerable to oxygen and thus appears more attractive for large-scale polymer production. Proposed by Percec and co-workers, SET-LRP mechanism involves an activator Cu^{0}, in powder or wire form, which promotes a heterolytic C-X bond cleavage of an initiator and a dormant polymer chain *via* an outer-sphere electron transfer to produce $Cu^{I}X/L$ and the propagating radical (R•). (Scheme 1) The key step in this mechanism is disproportionation of the *in-situ* generated $Cu^{I}X/L$ into the activator Cu^{0}/L and the deactivator $Cu^{II}X_2/L$. The $Cu^{II}X_2/L$ species reversibly deactivates R• to produce the dormant species R-X and regenerate $Cu^{I}X/L$. However, an alternative mechanism proposed by Matyjaszewski is called activators regenerated by electron transfer (ARGET) ATRP.[14-20] In this mechanism, $Cu^{I}X/L$ activates alkyl halides to give the propagating radicals (R•) while Cu^{0} serves as a heterogeneous reducing agent converting the persistent radical $Cu^{II}X_2/L$ to the activator $Cu^{I}X/L$. Furthermore, Cu^{0} may also react directly with alkyl halides to give $Cu^{I}X/L$ and R•.[21-23] Generally for both mechanisms, Cu^{0} acts as oxygen scavenger making this radical polymerization system less sensitive to air.[14,24-29]

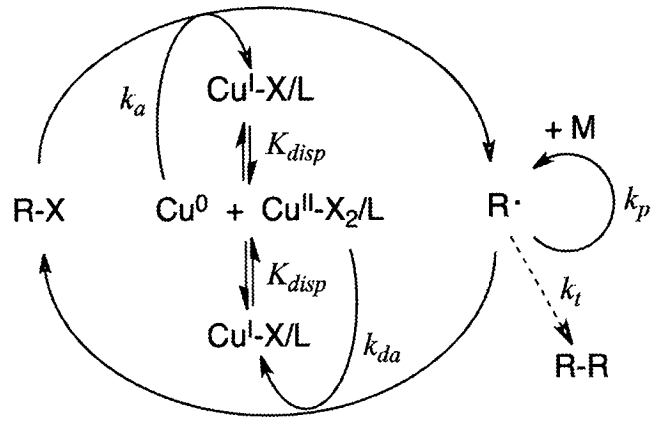

Scheme 1. Proposed Mechanism for SET-LRP.

We have been interested in investigating triazole-based compounds as catalyst supports in copper-catalyzed ATRP. Despite the well-established chemistry of the copper-catalyzed azide-alkyne cycloadditon (CuAAC), applications of its 1,2,3-triazole products as ligands in catalysis are relatively limited.[30-36] Although previous studies have employed the CuAAC in polymer synthesis,[37] only several examples of Cu catalysts supported by 1,2,3-triazole ligands in radical polymer synthesis are known.[38,39] In SET-LRP, ligands are expected to influence the disproportionation equilibrium of Cu^IX/L and stabilize the colloidal Cu^0 activator.[5] Despite these crucial roles, not many N-ligand types have so far been investigated.[40] Since the substituents at the triazole ring can be conveniently varied depending organic azides and terminal alkynes used, solubility and redox properties of the copper complexes can be systematically tuned and, as a result, the polymer properties can be manipulated. Our group has recently reported the use of the tripodaltriazole-based ligands tris(4-R-1,2,3-triazolylmethyl)amine [R = CH_2Ph (TBTA), CH_2Fc (TFcTA)] for copper-catalyzed normal ATRP.[39] However, a major drawback involving the Cu^IBr/TBTA and Cu^IBr/TFcTA catalysts was their low solubility in organic solvents, resulting in broad M_w/M_n values of the resulting polymers. To improve the catalyst's solubility in organic medium and increase the electron-donating ability, the more hydrophobic, tripodaltris(4-trimethylsilylmethyl-1,2,3-triazolylmethyl)amine (TTTA) was prepared and evaluated as a support for Cu(II) deactivator in SET-LRP of MMA.

Experimental

Materials

Methyl methacrylate (MMA; Merck, 99%) was dried with CaH_2 at room temperature for 2 d, distilled under vacuum, and stored in a teflon valve-sealed storage flask at -5 °C. Copper

metal was scrubbed with sandpaper, washed with hexane, and dried in an oven prior to use. Anisole (Anisole) was refluxed with Na under Ar and distilled under reduced pressure. DMSO (Lab Scan) was dried with CaH_2 and distilled under Ar. $TMSCH_2N_3$ was prepared according to the previous literature report.[41] $CuBr_2$ (Aldrich), tripropargyl amine (Aldrich), $TMSCH_2Cl$ (Merck), NaN_3 (Carlo Erba), ethyl-2-bromoisobutyrate (EBiB; Aldrich), and L(+)-ascorbic acid (Riedel-de Haën) were purchased and used as received.

^1H (500 MHz), $^{13}C\{^1H\}$ (125 MHz), and $^{29}Si\{^1H\}$ (99 MHz) NMR spectra were acquired on Bruker AV-500 spectrometer equipped with a 5 mm proton/BBI probe. All NMR spectra were recorded at room temperature and referenced to protic impurities in the deuterated solvent for ^1H, solvent peaks for $^{13}C\{^1H\}$, and $Si(CH_3)_4$ for $^{29}Si\{^1H\}$. Elemental analyses were conducted by Chemistry Department, Mahidol University.

Synthesis and Characterization

Tris(4-trimethylsilylmethyl-1,2,3-triazolylmethyl)amine (TTTA). Tripropargyl amine (0.91 mL, 6.4 mmol) was treated with 3.3 equiv of $TMSCH_2N_3$ (2.8 g, 22 mmol) in a 1:1 mixture of CH_2Cl_2:H_2O (50 mL) with 15 mol% of $CuSO_4 \cdot 5H_2O$ (1.0 M, 1.0 mL, 1.0 mmol) and 45 mol% of ascorbic acid (0.51 g, 2.9 mmol). After 24 h, 30 mL of distilled water was added to the reaction mixture after which the aqueous layer was extracted with 3x30 mL of CH_2Cl_2. To the combined organic layer was added EDTA (0.32 g, 1.1 mmol) in 10% aqueous solution of NH_3 (170 mL). The resulting mixture was stirred for 3 h and the CH_2Cl_2 solution was washed with 3x30 mL of distilled water. Then, the CH_2Cl_2 solution was dried over anhydrous Na_2SO_4. Recrystallization in diethyl ether afforded the product TTTA in 74% yield (2.4 g, 4.7 mmol). ^1H NMR (500 MHz, $CDCl_3$, δ): 7.65 (s, 3H; C*H*=), 3.91 (s, 6H; NCH_2), 3.71 (s, 6H; CH_2Si), 0.13 (s, 27H; SiCH_3). $^{13}C\{^1H\}$ NMR (125 MHz, $CDCl_3$, δ): 143.5, 124.4 (triazole carbons), 46.9 (CH_2), 41.8 (CH_2), 2.6 (CH_3). $^{29}Si\{^1H\}$ NMR (99 MHz, $CDCl_3$, δ): 2.3 (s). Anal.Calcd for $C_{21}H_{42}N_{10}Si_3$: C 48.61, H 8.16, N 26.99; found: C 48.27, H 8.10, N 27.12.

$CuBr_2$(TTTA). Reaction of TTTA (0.20 g, 0.38 mmol) with $CuBr_2$ (0.094 g, 0.42 mmol) was carried out in CH_2Cl_2 under Ar at room temperature. After 5 h, the dark green solution was dried *in vacuo*. Recrystallization in ethyl acetate resulted in a green, microcrystalline solid in 57% yield (0.18 g, 0.24 mmol). ^1H NMR (500 MHz, $CDCl_3$, δ): 4.20 (br s, 6H; CH_2Si), 0.22 (br s, 27H; SiCH_3). $^{29}Si\{^1H\}$ NMR (99 MHz, $CDCl_3$, δ): -7.0 (s). Anal.Calcd for $C_{21}H_{42}N_{10}Br_2CuSi_3$: C 33.98, H 5.70, N 18.87; found: C 33.90, H 5.63, N 18.77.

Cyclic Voltammetry

A voltammogram was recorded at ambient temperatures with Autolab PGSTAT 30 potentiostat and GPES software. The Cu^{II} complex $CuBr_2$/TTTA (1.0 mM) was dissolved in dry DMSO containing 0.1 M $[Et_4N][PF_6]$ electrolyte. Measurements were performed under Ar at a scanning rate of 0.01 V s^{-1} with a glassy carbon working electrode, a platinum counter electrode, and a Ag/Ag^+ reference electrode. The sample was referenced to the ferrocene internal standard and its potential was reported *versus* those of Fc/Fc^+.

General Procedure for SET-LRP of MMA

To a dried Schlenk tube equipped with a magnetic stir bar was added TTTA (48 mg, 0.093 mmol) and $CuBr_2$ (21 mg, 0.093 mmol) under Ar. Then, 2.0 mL of MMA (19 mmol) was added. The reaction flask was tightly closed and the solution mixture was degassed by three freeze-pump-thaw cycles using dry ice/acetone. Under an Ar flow, a copper sheet (size = 0.5x0.5, 1.0x1.0, or 1.5x1.5 cm^2) was added to the frozen reaction mixture after which the system was evacuated and refilled with Ar five times. Next, the reaction mixture was allowed to thaw, to which anisole (200 μL), used as an internal standard, was added. After 10 min at room temperature, ethyl-2-bromoisobutyrate (30 μL, 0.19 mmol) was added via a syringe to initiate the polymerization. The reaction flask was immediately immersed in a pre-heated oil bath. After a given time, approximately 20 mL of THF was added to stop the polymerization, after which the Schlenk tube was cooled at -78 °C for 5 min. The resulting polymer was precipitated out using *ca.* 200 mL of CH_3OH.

SET-LRP of MMA in the Presence of Air

Polymerizations with added air followed the general procedure for SET-LRP. A certain volume of air was introduced to the reaction flask *via* a syringe immediately after immersing the reaction tube in the pre-heated oil bath. The septum was then wrapped with electrical tape and Parafilm®. In case of polymerizations under aerobic conditions, the reaction mixture was not degassed by the freeze-pump-thaw technique and the polymerization was carried out in air.

Polymerization Characterizations

Based on ^1H NMR spectroscopy, monomer conversions were determined by comparing the $-OCH_3$ peak area of PMMA to the $-OCH_3$ integration of the anisole reference. Molecular weight distributions of polymer were measured using a Waters e2695 system equipped with PLgel 10-mm mixed B 2 columns (molecular weight resolving range = 500–10,000). As eluent, THF was used at a flow rate of 1 mL/min at 40 °C with a calibration based on poly(methyl methacrylate) (PMMA) standards.

Kinetic Experiments

Kinetic studies were performed in neat MMA under similar conditions as described for SET-LRP, except that the amounts used was three times that of typical SET-LRP (0.28 mmol of $CuBr_2$ and TTTA, three appropriately sized copper sheets, 600 μL of anisole, 6.0 mL of MMA, and 90 μL of EBiB). After a given time, approximately 0.5 mL of a sample was withdrawn using a syringe to determine monomer conversions, polymer molecular weights, and PDI values via ^1H NMR spectroscopy and GPC analysis, respectively.

Results and Discussion

Synthesis of Tripodal Click Ligand (TTTA) and the $CuBr_2$/TTTA Complex

Reaction of $N(CH_2CCH)_3$ and 3 equiv of $Me_3SiCH_2N_3$ in a 1:1 mixture of CH_2Cl_2:H_2O at room temperature afforded tris(4-trimethylsilylmethyl-1,2,3-triazolylmethyl)amine (TTTA) as a white solid which was crystallized from diethyl ether in 74% yield (Scheme 2). The ^1H NMR spectrum of TTTA ($CDCl_3$) contains a characteristic C*H* (triazole) singlet resonance at δ 7.9 whereas the $SiMe_3$ group appears at δ 0.16 and δ 2.3 in the ^1H NMR and $^{29}Si\{^1H\}$ NMR spectra, respectively.

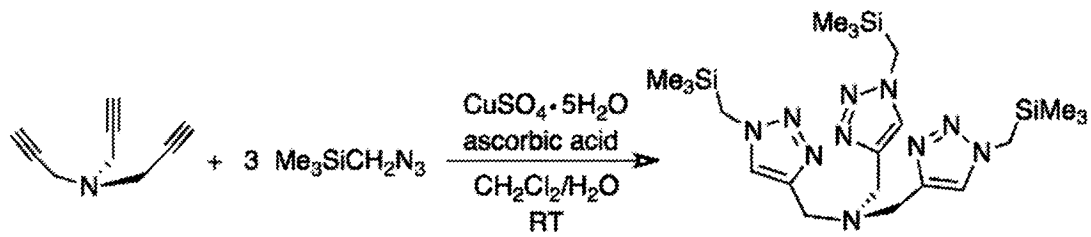

Scheme 2. Synthesis of tris(4-trimethylsilylmethyl-1,2,3-triazolylmethyl)amine (TTTA).

Treatment of TTTA with one equiv of $CuBr_2$ in CH_2Cl_2 at room temperature readily produced the corresponding dark green Cu^{II} complex $CuBr_2$/TTTA. Crystallization of $CuBr_2$/TTTA in ethyl acetate afforded a green microcrystalline solid in 57% yield. Due to the paramagnetic nature of the Cu^{II} complex, its ^1H NMR spectrum in $CDCl_3$ reveals broad resonances at δ 4.2 and δ 0.22, corresponding to CH_2Si and $Si(CH_3)_3$, respectively. The $^{29}Si\{^1H\}$ NMR spectrum contains a singlet resonance at δ -7.0. It should be noted that crystal structure of the related complex $[Cu^{II}Cl(TBTA)][Cl]$ has previously been reported showing a distorted trigonalbipyramidal structure with an outer-sphere chloride ion.[42]

Table 1. CV data of $CuBr_2$/L in DMSO.[a]

Entry	Complex	$E_{p,a}$ [V]	$E_{p,c}$ [V]	ΔE_p [mV]	$E_{1/2}$[b] [V]
1	$CuBr_2$/TTTA	-0.206	-0.338	132	-0.272
2[c]	$CuBr_2$/TBTA	-0.0885	-0.324	235	-0.206
3[c,d]	$CuBr_2$/TFcTA	-0.0625	-0.386	324	-0.224

[a] 0.1 M $[NBu_4][PF_6]$, 1.0 mM $CuBr_2$/L, scan rate 0.01 V s^{-1}, potentials reported *versus* Fc/Fc^+, $E_{p,a}$ and $E_{p,c}$ are the peak potentials of the oxidation and reduction waves, respectively. [b] $E_{1/2} = (E_{p,a} + E_{p,c})/2$. [c] ref.39 [d] Fe(II)/Fe(III) redox potentials of the ferrocenyl substituents are not shown.

Cyclic voltammetry (CV) of $CuBr_2$/TTTA was measured in DMSO and referenced to the ferrocene internal standard. The CV profile of $CuBr_2$/TTTA reveals a quasi-reversible Cu^I/Cu^{II} redox wave at $E_{1/2}$ = -0.272 V with the cathodic-anodic peak separation (ΔE_P) of 132 mV (entry 1, Table 1). In comparison to the previously reported values of tripodal click analogues tris(4-R-1,2,3-triazolylmethyl)amine [R = $-CH_2C_6H_5$ (TBTA) and $-CH_2Fc$ (TFcTA); entries 2 and 3, Table 1], the TMS-substituted tripodal ligand (TTTA) exhibited stronger electron-donating property based on a lower $E_{1/2}$value.

SET-LRP of MMA with Cu^0/$CuBr_2$/TTTA

Bulk polymerizations of MMA were catalyzed by a 1.0x1.0 cm^2 Cu^0 sheet ($[Cu^0]$ = 0.90 cm^2/mL) in the presence of $CuBr_2$/TTTA using the molar ratio of $[MMA]_0/[EBiB]_0/[CuBr_2]_0/[TTTA]_0$ = 200/2/1/1. Heating the reaction mixture at 90 °C initially resulted in a homogeneous green solution, indicative of Cu^{II} species. After a while, the polymerization mixture turned slightly cloudy and pale yellow in color, which could be attributed to the *in-situ* reduction of Cu^{II} to Cu^I species. It was found that, in the presence of TTTA ligand, an effective SET-LRP of MMA in bulk was achieved as 76% yield of PMMA (PDI = 1.19) was obtained (entry 2, Table 2).

Table 2. SET-LRP of MMA using different amounts of Cu^0, $Cu^{II}Br_2$, EBiB, and TTTA.[a]

Entry	MMA	EBiB	Cu^0 sheet [cm^2]	Time [h]	Conv. [%]	$M_{n,th}$[b]	$M_{n,GPC}$	PDI
1[c]	200	2	1.0x1.0	5.0	75	7 704	47 700	1.55
2	200	2	0.5x0.5[d]	5.0	82	8 405	18 400	1.16
3	200	2	1.0x1.0[e]	3.5	76	7 758	24 200	1.19
4	200	2	1.5x1.5[f]	2.8	68	7 038	29 500	1.13
5	400	2	1.0x1.0	3.5	76	15 413	26 200	1.25
6	400	4	1.0x1.0	6.0	85	5 802	11 700	1.37
7	1000	2	1.0x1.0	8.0	53	26 652	40 200	1.30
8	1000	10	1.0x1.0	11	45	4 700	8 200	1.35
9	2000	2	1.0x1.0	15	45	45 249	48 100	1.37
10[g]	2000	2	1.0x1.0	19	64	64 272	123 300	1.39

[a] Polymerization conditions: 90 °C, ethyl-2-bromoisobutyrate (EBiB), molar ratio $[MMA]_0/[EBiB]_0/[CuBr_2]_0/[TTTA]_0$ = MMA/EBiB/1/1. [b] $M_{n,th} = [([MMA]_0/[EBiB]_0) \times \%\ \text{conversion} \times M_{w,MMA}] + M_{w,EBiB}$. [c] no $CuBr_2$ added. [d] $[Cu^0] = 2.0\ cm^2/mL$. [e] $[Cu^0] = 0.90\ cm^2/mL$. [f] $[Cu^0] = 0.22\ cm^2/mL$. [g] $[MMA]_0/[EBiB]_0/[CuBr_2]_0/[TTTA]_0$ = 2000/2/1/3.

When the $Cu^{I}Br$/TTTA catalyst was used, a negligible amount of polymer product was isolated after 24 h. On the other hand, without $Cu^{II}Br_2$, the Cu^0/TTTA catalyst system resulted in poorly controlled polymerization with high polymer mass and M_w/M_n value (entry 1). Based on these results, Cu^0 is proposed as the active catalyst, which directly activates the C-Br bond, whereas the deactivator $Cu^{II}Br_2$ is crucial to achieve well-controlled polymerizations.

The effect of Cu^0 areas was investigated, as shown in entries 2–4 (Table 2). While the polymerization systems using 1.5x1.5 cm^2 ($[Cu^0] = 2.0\ cm^2/mL$) and 1.0x1.0 cm^2 ($[Cu^0] = 0.90\ cm^2/mL$) Cu^0 sheets resulted in similar polymer yields, the smaller Cu^0 area of 0.5x0.5 cm^2 ($[Cu^0] = 0.22\ cm^2/mL$) afforded slower polymerization. This observation was supported by kinetic studies, which revealed first-order kinetic plots and comparable observed polymerization rate constants ($k_{obs} \sim 1.2x10^{-4}\ s^{-1}$) for all three different Cu^0 surface areas (Figure 1). Although several previous studies have shown that increasing the amount of Cu^0 generally gave higher k_{obs} values,[14,43,44] Percec and co-workers have recently reported similar

finding in which k_{obs} values were not significantly affected by the changes in Cu^0 surface area.[45] It was possible that, under the polymerization conditions studied, the solution was already saturated with the active Cu^0 catalyst. The kinetic plots shown in Figure 1 also revealed that the smallest Cu^0 area of 0.50x0.50 cm^2 ($[Cu^0]$ = 0.22 cm^2/mL) afforded a longer induction period (52 min). On contrary, polymerization systems with 1.0x1.0 cm^2 and 1.5x1.5 cm^2 copper sheets ($[Cu^0]$ = 0.90 cm^2/mL and 2.0 cm^2/mL, respectively) surprisingly resulted in similar induction periods (*ca.* 8 min). The reason for the discrepancy involving comparable induction periods for different Cu^0 surface areas (entries 3 and 4) is still unclear and will be subjected to further study.

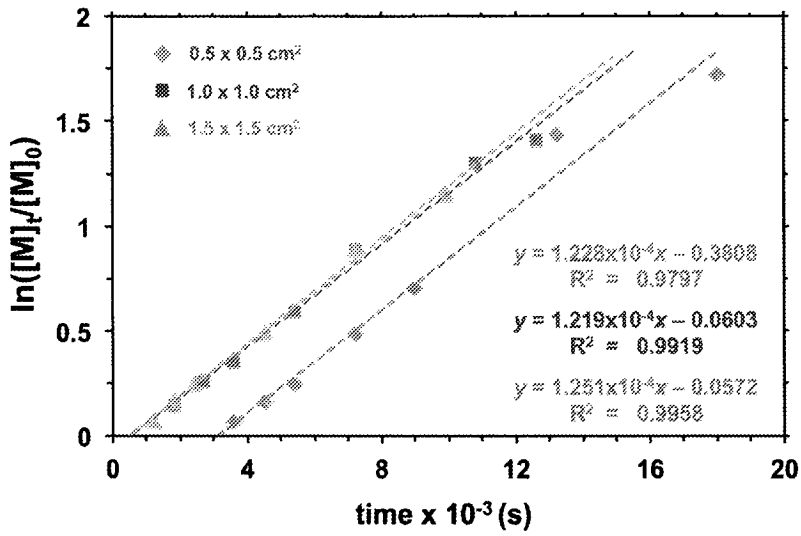

Figure 1. Kinetic plots of bulk polymerizations of MMA as a function of Cu^0 area (0.5x0.5 cm^2, 1.0x1.0 cm^2, 1.5x1.5 cm^2).

Effect of Copper Concentration

Due to the heterogeneity nature of SET-LRP,it should be possible to use a low starting amount of the catalyst system $Cu^0/CuBr_2$/TTTA.[46-48] To investigate the effect of the amount of copper catalyst, higher monomer ratios of $[MMA]_0/[CuBr_2]_0/[TTTA]_0$ (400/1/1, 1000/1/1, and 2000/1/1) were used in the presence of a 1.0x1.0 cm^2 copper sheet. The polymerization data revealed that a decrease in $CuBr_2$/TTTA concentrations (500–50 ppm) and $[Cu^0]$ (0.47–0.099 cm^2/mL) resulted in slower and less controlled polymerizations (PDI = 1.25–1.39) (entries 5–10, Table 2). An increase in the $[EBiB]_0/[MMA]_0$ ratio afforded no change in the polymerizations although lower polymer molecular weights were obtained (entries 6 and 8). Along the same line, the use of a 3-fold excess of TTTA did not have an apparent effect on the polymerization nor the polymer M_w/M_n value (entry 10).

Effect of Added Air

Catalyst tolerance to oxygen was important for the industrialization of ATRP. Thus, controlled radical polymerizations in the presence of air were evaluated for this catalyst system. In general, oxygen from air was known to oxidize Cu^{I} to the deactivator species $Cu^{II}Br_2$/L and consequently slowed down the polymerization rates. Table 3 has shown that higher amounts of injected air (*i.e.*, 1.0, 3.0, and 5.0 mL, entries 1–3) indeed led to reduced monomer conversions at 3 h although the polymerizations remained well controlled based on low M_w/M_n values in the range of 1.12–1.25. In fact, for entry 4, MMA was polymerized under aerobic conditions using non-degassed MMA. In the presence of oxygen and moisture, the polymerization was slow and the reaction mixture appeared viscous after 9 h. Despite relatively low monomer conversion (53%), the narrow polymer M_w/M_n value of 1.21 was obtained, based on ^{1}H NMR and GPC spectra.

Table 3. Effect of added air on SET-LRP of MMA using $Cu^0/Cu^{II}Br_2$/TTTA.[a]

Entry	air [mL]	Time [h]	Conv. [%]	$M_{n,th}$[b]	$M_{n,GPC}$	PDI
1	1.0	3.0	64	6 556	17 300	1.14
2	3.0	3.0	44	4 609	14 600	1.12
3	5.0	3.0	19	2 105	5 900	1.25
4	in air	9.0	53	5 573	22 900	1.21

[a] Polymerization conditions: 90 °C, initiator = ethyl-2-bromoisobutyrate (EBiB), $[Cu^0]$ = 0.90 cm^2/mL, molar ratio $[MMA]_0/[EBiB]_0/[CuBr_2]_0/[TTTA]_0$ = 200/2/1/1 in bulk MMA. [b] $M_{n,th} = [([MMA]_0/[EBiB]_0) \times \%\ \text{conversion} \times M_{w,MMA}] + M_{w,EBiB}$.

Effect of Temperature and Activation Energy

The effect of temperatures on catalyst activity and polymer property was studied by varying polymerization temperatures (*i.e.*, 40–90 °C). Figure 2 showed that, in all cases, the first-order kinetic plots were obtained. In addition, observed rate constants of polymerization (k_{obs}) decreased at lower temperatures (Table 4). For temperatures investigated, an induction period was present and found to be longer as the polymerization temperatures decreased. For example, at 90 °C, the induction period was 8 min compared to 14 h at 40 °C.

Table 4. Effect of reaction temperature on SET-LRP of MMA using $Cu^{0}/Cu^{II}Br_2$/TTTA.[a]

Entry	Temp. [°C]	Time [h]	Conv. [%]	$M_{n,th}$[b]	$M_{n,GPC}$	f[c]	PDI	k_{obs} [s^{-1}]
1	90	3.5	76	7 758	24 200	0.32	1.19	1.22×10^{-4}
2	80	4.0	62	6 387	20 600	0.31	1.23	8.12×10^{-5}
3	60	6.0	52	5 427	35 900	0.15	1.30	4.02×10^{-5}
4	40	38	42	4 393	57 000	0.08	1.40	6.24×10^{-6}

[a] Polymerization conditions: 90 °C, initiator = ethyl-2-bromoisobutyrate (EBiB), $[Cu^{0}]$ = 0.90 cm^2/mL, molar ratio $[MMA]_0/[EBiB]_0/[CuBr_2]_0/[TTTA]_0$ = 200/2/1/1 in bulk MMA. [b] $M_{n,th}$ = $[([MMA]_0/[EBiB]_0)$ x % conversion x $M_{w,MMA}] + M_{w,EBiB}$. [c] f (initiation efficiency) = $M_{n,th}/M_{n,GPC}$.

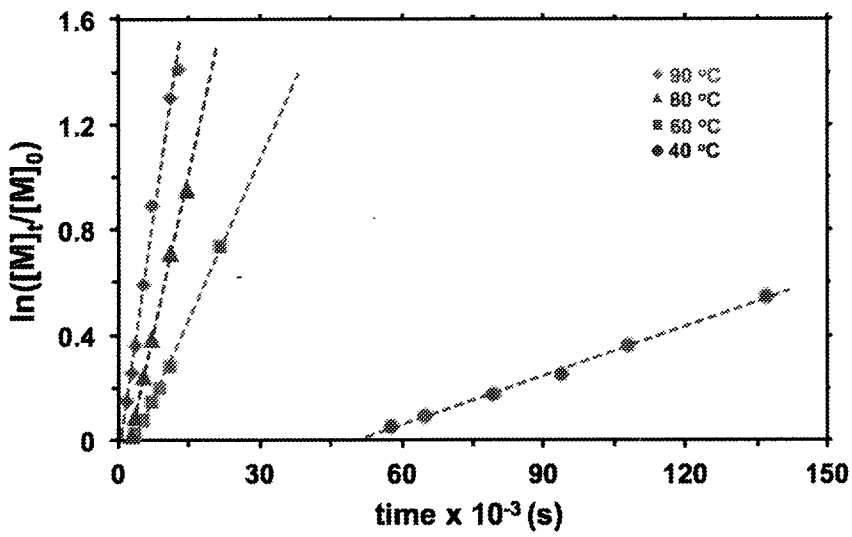

Figure 2. Kinetic plots of bulk polymerizations of MMA as a function of reaction temperature (90 °C, 80 °C, 60 °C, 40 °C).

Based on these data, the Arrhenius plot of $\ln(k_{obs}/T)$ *vs.* 1/T in the temperature range of 40–90 °C was constructed as illustrated in Figure 3, giving the calculated activation energy (E_a) of 22.6 kJ/mol. To the best of our knowledge, this is the first report of an apparent energy of activation of copper-mediated SET-LRP system. However, there are previous reports of E_a values of normal copper-catalyzed ATRP of MMA. For example, Sivaram and co-workers found the apparent activation energy of the $Cu^{I}Br$/BPIEP catalyst (BPIEP = 2,6-bis[1-(2,6-diisopropylphenyl- imino)ethyl]pyridine) for normal ATRP of MMA in toluene to be 51.0 kJ/mol.[49] Several other examples of E_a values for normal ATRP of MMA appeared to be

similar in the range of 53–63 kJ/mol.[50-53] The low E_a value of 21.7 kJ/mol was obtained for normal ATRP of MMA catalyzed by CuBr with the bidentate, cyclopentyl-substituted pyridine-2-carboximidate ligand in 50 wt% veratrole solution.[54] On the basis of these values, the apparent activation energy of bulk polymerizations of MMA using the catalyst system $Cu^0/CuBr_2$/TTTA is considered very low, consistent with observed high catalyst activity compared to other ATRP systems.

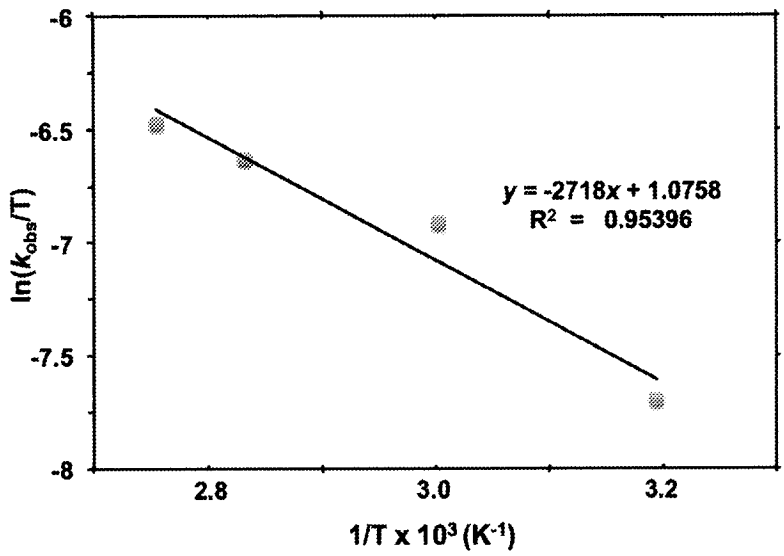

Figure 3. An Arrhenius plot in the temperature range of 40–90 °C.

Conclusion

We have demonstrated that tris(4-trimethylsilylmethyl-1,2,3-triazolylmethyl)amine (TTTA) is an effective ligand for copper-catalyzed SET-LRP of MMA. In this work, the k_{obs} values were found to be independent of the Cu^0 surface area, possibly due to saturation of Cu^0 active species under the experimental conditions investigated. Bulk polymerizations of MMA in the presence of air were slow but well controlled, as evidenced by narrow polymer PDI values. Kinetic data from the polymerization temperature range of 40–90 °C revealed longer induction periods with decreasing temperatures and relatively low apparent activation energy (E_a = 22.6 kJ/mol). These promising polymerization results coupled with an ease of ligand synthesis and modification make the tripodaltriazole-based derivative of the type tris(4-R-1,2,3-triazolylmethyl)amine an attractive ligand class for copper-catalyzed SET-LRP. Further modification of substituents at the triazole ring and optimization of polymerization conditions in order to improve monomer conversion and initiation efficiency of the system are ongoing.